

Study of galaxies in the Lynx-Cancer void. I. Sample description

S. A. Pustilnik,^{1,2*} and A. L. Tepliakova^{1*}

¹ *Special Astrophysical Observatory of RAS, Nizhniy Arkhyz, Karachai-Circassia 369167, Russia*

² *Isaac Newton Institute of Chile, SAO branch, Nizhniy Arkhyz, 369167, Russia*

Accepted April 2011 28; Received July, 2010

ABSTRACT

The evolution of galaxies is influenced by the environment in which they reside. This effect should be strongest for the least-mass and -luminosity galaxies. To study dwarf galaxies in extremely low density environments we have compiled a deep catalogue of dwarf galaxies in the nearby Lynx-Cancer void. This void hosts some of the most metal-poor dwarfs known to date. It borders the Local Volume at the negative supergalactic $Z(SGZ)$ coordinates and has the size of more than 16 Mpc. With a distance to its centre of only 18 Mpc it is close enough to allow the search for the faintest dwarfs. Within the void 75 dwarf ($-11.9 > M_B > -18.0$) and 4 subluminoous ($-18.0 > M_B > -18.4$) galaxies have been identified. We present the parameters of the void galaxies and give a detailed analysis of the completeness of the catalogue as a function of magnitude and surface brightness. The catalogue appears almost complete to $M_B < -14$ mag, but misses part of the fainter low surface brightness (LSB) face-on galaxies. This sample of void galaxies builds the basis of forthcoming observational studies that will give insight into the main stellar population, HI-mass-to-light ratio, metallicity and age for comparison with dwarfs in higher density regions. We briefly summarize the information on the unusual objects in the void and conclude that their concentration hints that voids are environments that are favourable for finding and studying unevolved dwarf galaxies.

Key words: galaxies: dwarf – galaxies: evolution – galaxies: distances and redshifts – galaxies: luminosity function – large-scale structure of Universe

1 INTRODUCTION

The modern models of large-scale structure and galaxy formation, including the state-of-art N-body simulations, predict that galaxy properties and evolution significantly depend on global environment (e.g. Peebles 2001; Mathis & White 2002; Tully et al. 2002; Gottlöber et al. 2003; Hoefl et al. 2006; Arhipova et al. 2007; Hahn et al. 2007, 2009, and references therein). While the effect of a denser environment on galaxy properties and evolution has been known for a rather long time (e.g. Haynes, Giovanelli & Chincarini 1984; Boselli & Gavazzi 2006), the role of the most rarefied environment such as voids on galaxy formation and evolution is less studied, either theoretically and observationally.

The latter is due to observational selection effects. Most galaxies with known radial velocities are found in spectral surveys of magnitude-limited samples. Wide-field spectral surveys have typical apparent magnitude limits cor-

responding roughly to $B \sim 18$ mag. This apparent magnitude limit implies that for distances well beyond the Local Supercluster ($cz > 5000 - 6000 \text{ km s}^{-1}$), where the great majority of large voids (with sizes of 20–40 Mpc) were found, the faintest selected galaxies will have absolute magnitudes M_B of ~ -16 mag or brighter. This implies that the study of distant voids is limited to galaxies $\sim 3-4$ mag fainter than L^* galaxies ($M_B^* \approx -19.5$ to -20.0 mag). L^* galaxies are typically the ones that mark the borders of voids. Therefore, even the most advanced studies of the void galaxy population, based on very large samples with redshifts from the Sloan Digital Sky Survey (SDSS) (e.g. Sorrentino, Antonuccio-Delogu & Rifatto 2006; Patiri et al. 2006) of $z < 0.03-0.05$ ($M_r \lesssim -20.0$), were limited to galaxies with luminosities of only ~ 2 magnitudes fainter than M_r^* . Only studies of photometric and spectroscopic properties for SDSS samples with $z < 0.025$, $M_r \lesssim -14.0$ (Rojas et al. 2004, 2005) were able to probe less luminous galaxies. A new detailed study of the properties of galaxies in voids, described by Stanonik et al. (2010) and

* sap@sao.ru (SAP), arina@sao.ru (ALT)

van de Weygaert et al. (2009) also mainly deals with more luminous dwarf galaxies, namely with $M_R < -16.0$ mag.

The smaller a galaxy, the more fragile it is in respect to external disturbance. Therefore, the possible difference of galaxy properties in various types of environments is expected to depend on galaxy mass. Thus, the relatively ‘shallow’ probes of ‘distant’ void galaxy population based on the SDSS samples leave significant room for deeper insight into the question.

Earlier studies found galaxies in voids to typically be low-mass actively star-forming galaxies, like BCGs and HII galaxies (in particular, Salzer 1989; Pustilnik et al. 1995; Popescu, Hopp & Elsässer 1997). Lindner et al. (1996) have shown that BCGs are not the only objects in voids. More typical dwarfs with lower star formation (SF) activity also populate voids. Statistical studies of optical properties of void galaxies in the SDSS data did not provide further clues to the evolutionary state of these galaxies, but confirmed the increased fraction of blue galaxies and Star Formation Rate (SFR). The only proxy of evolutionary parameters for void galaxies studied up to now, is the ratio $M(HI)/L_B$, but only for a limited sample of BCGs (Pustilnik et al. 2002). The recent study of void galaxies via HI imaging by Stanonik et al. (2010) is less selective, but still is rather limited with regard to luminosity.

The amount of evidence that BCGs in underdense regions may represent a less evolved population was growing during the last decade (e.g. Peebles 2001; Pustilnik et al. 2003, 2004, 2006). However, this might be due to selection effects which favour actively star-forming galaxies. Therefore, there is a need to address this issue by defining samples that also contain the more typical late-type galaxies, particularly because void environments are thought to be favourable for sufficiently quiet galaxy evolution. Hence, one can hope to use the statistics of void galaxy ensembles as a good instrument for comparison with predictions of cosmological galaxy formation scenarios. Such large and deep samples of void galaxies would also allow a more detailed comparison with predictions from cosmological N-body simulations (e.g. Tikhonov & Klypin 2009).

To construct void galaxy samples with absolute magnitudes down to $M_B \sim -12$, from samples with the typical apparent magnitude limit of $m_B \sim 18-19$, one needs to limit the distant boundary by $D \sim 10-16$ Mpc. The nearest voids (e.g. Fairall 1998), adjacent to the Local Volume (distances of <10 Mpc, as defined, e.g. by Karachentsev et al. 2004) are suitable for this task. Due to their relative proximity ($D_{\text{centre}} \sim 10-15$ Mpc), the low-luminosity galaxies can be relatively easily identified. Moreover, spectroscopic studies of their element abundances in the relatively faint HII regions of these fairly nearby galaxies is feasible with modern large telescopes.

In this paper we present the sample of galaxies residing in one of the nearest, Lynx-Cancer, voids mentioned in Pustilnik et al. (2003). The choice of the void is motivated by a good coverage of this sky region by the SDSS spectral and image databases (Fukugita et al. 1996; Gunn et al. 2003; York et al. 2000; Smith et al. 2002; Pier et al. 2003), which leads to a significant increase in the number of known void galaxies and provides the photometric properties of the void galaxies. The study of this sample is also motivated by the prominent concentration of atypical dwarf

galaxies in this volume. Half a dozen objects in this relatively modest void are very metal-poor galaxies and/or reveal no visible old stellar population (Pustilnik et al. 2003; Pustilnik, Kniazev & Pramskij 2005a; Pustilnik et al. 2010, Pustilnik et al. 2011, MNRAS, submitted).

The lay-out of the paper is as follows. In Section 2 we summarize information on the nearby voids, and describe the Lynx-Cancer void. Section 3 presents the void galaxy sample. In Section 4 we discuss the completeness of the void galaxy sample, summarize the properties of the most unusual void galaxies and the prospects to increase this galaxy sample with LSB dwarf galaxies that are missed in the SDSS spectral database. Section 5 presents the summary of the main results. We adopt the value of Hubble constant as $H_0=73 \text{ km s}^{-1} \text{ Mpc}^{-1}$.

2 NEARBY VOIDS. THE LYNX-CANCER VOID DESCRIPTION

2.1 Nearby voids

The issue of the nearest voids was briefly addressed by Fairall (1998). In Table 1 we summarise (ranked on the void size, apart from the Lynx-Cancer subvoid) and update on the main parameters of the nearby voids. In comparison to the original Fairall (1998) list, the Inner Local Void from Tully et al. (2008) is added. The misprint is corrected for RA of the Monoceros void centre (A. Fairall, private communication) and for all the related parameters as well. Finally, the Lynx-Cancer void and its subvoid are added with their parameters. The void maximal extent in units of km s^{-1} is shown in column 2. In columns 3 and 4 we present the approximate equatorial coordinates of the void centres. Column 5 gives the distances to the void centres (cz relative to the restframe of the Local Group in km s^{-1}). In columns 6 and 7 the Galactic longitudes and latitudes of the void centres are given, respectively, while columns 8, 9 and 10 present their approximate supergalactic X, Y and Z coordinates, respectively.

The giant Local Void described by Tully et al. (2008) begins close to the Local Group and its neighbouring groups at the positive supergalactic Z . The Local Void appears pretty empty. Its expected population of dwarf galaxies remains almost elusive. Whether this is the effect of obscuration by the Galaxy disc or the intrinsic property of the Local Void, or the combination of both, remains unclear. While other nearby voids are also interesting for detailed studies of their galaxy population, we concentrate here on the Lynx-Cancer void.

The Lynx-Cancer void was discovered as a result of a study of the very low-metallicity BCG HS 0822+3542 (one of many such galaxies found in the Hamburg-SAO Survey; Ugryumov et al. 1999; Pustilnik et al. 2005b, and references therein) and its companion, the LSB dwarf galaxy SAO 0822+3545. Pustilnik et al. (2003) noticed that they are situated in a very rarefied environment. This was the motivation for a more careful analysis of the galaxy content in this volume which led to the identification of another nearby void, similar to those described by Fairall (1998). This void is adjacent to the Monoceros void and they probably represent the parts of a larger ‘empty’ volume at the negative SGZ . In comparison to other nearby

Table 1. Parameters of the nearby voids

Designation	Size km s ⁻¹	RA hour	Dec °	<i>cz</i> km s ⁻¹	<i>l</i> °	<i>b</i> °	<i>SGX</i> km s ⁻¹	<i>SGY</i> km s ⁻¹	<i>SGZ</i> km s ⁻¹
Cetus	500	02.0	-20	700	192	-72	100	-600	-200
Cepheus	500	23.5	+65	800	112	+05	700	0	300
Crater	500	11.5	-15	1500	126	-28	1300	-700	200
Volans	700	07.0	-70	800	281	-25	-600	-300	-500
Monoceros	1000	08.0	+05	800	216	+17	200	430	-970
Lynx-Cancer main	1200	07.9	+27	1030	194	+25	660	660	-930
Lynx-Cancer subvoid	870	08.5	+29	770	195	+34	470	674	-680
Inner Local Void	2000	18.5	-01	900	30	+02	-500	-200	700

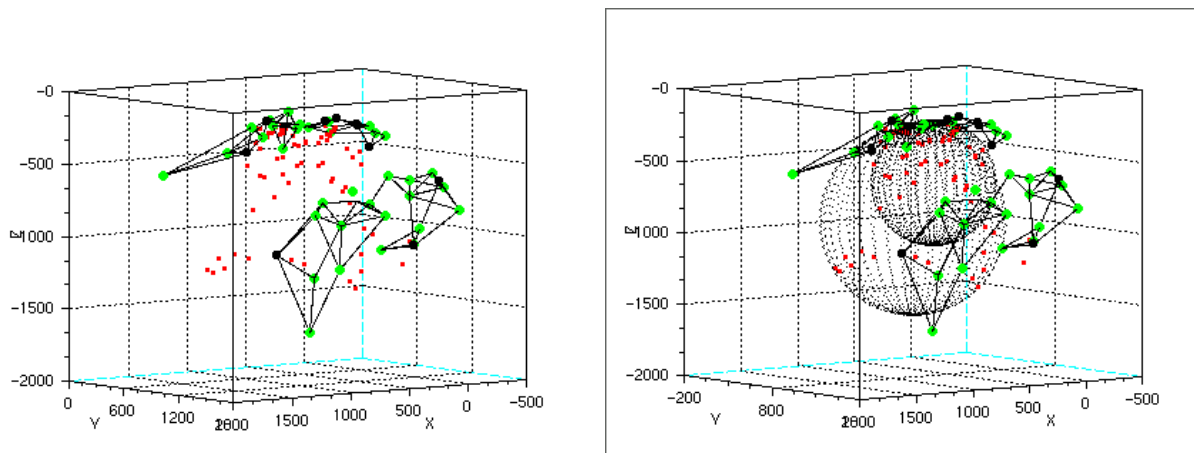


Figure 1. *Left panel:* the 3D view of the Lynx-Cancer void region with positions of ‘luminous’ galaxies ($M_B < -19.0$ mag). The supergalactic coordinate grid (SGX, SGY, SGZ) is in units of km s^{-1} . Large filled green dots show positions of pairs and groups in which at least one ‘luminous’ galaxy enters. Large black filled dots show positions of ‘isolated’ luminous galaxies. Each luminous galaxy is joined with the three the nearest luminous neighbours to help visually define the void border. Dwarf galaxies inside the void are shown by small red squares. *Right panel:* The same figure with a contour sketch of the larger main void (large sphere) and the subvoid (smaller sphere), suggested in Pustilnik et al. (2003), which includes a large fraction of void galaxies.

voids, the Lynx-Cancer void has two advantages: (a) the major part of the respective sky region is covered by the SDSS imaging and spectroscopy database (York et al. 2000; Abazajian et al. 2009, and references therein), and (b) a large part of this sky region will be covered by the blind high-sensitivity HI surveys, including the Arecibo survey ALFALFA (e.g. Haynes 2008), the Australian survey ASKAP (Johnston et al. 2008), the Westerbork survey Apertif (e.g. Oosterloo, Verheijen, van Cappelen 2008) and the Effelsberg survey EBHIS (e.g. Winkel et al. 2010).

Surprisingly, several other very metal-poor dwarf galaxies, including two objects with $Z \lesssim 1/30 Z_\odot$ [or $12 + \log(O/H) \lesssim 7.16$], were found in this volume (Pustilnik, Kniazev & Pramskij 2005a; Izotov & Thuan 2007; Pustilnik et al. 2010, see details in Section 4). These and other findings hint at the probable effect of the void environment on dwarf galaxy formation and evolution. However, to study the evolutionary status of void dwarf galaxies statistically, one needs to describe the void geometry and boundaries more carefully, to better define the dwarf galaxy sample falling within the void. The statistical approach also requires a well-defined control sample in regions of higher galaxy densities. Fortunately, the detailed

studies of a large number of dwarf galaxies have appeared recently, which can be used for comparison; such as the FIGGS sample of 65 faint ($M_B \gtrsim -15.7$) late-type dwarfs (Begum et al. 2008), of which $\sim 3/4$ belong to the Local Volume groups.

2.2 Luminous galaxies delineating the Lynx-Cancer void

We show the boundaries of the Lynx-Cancer void, as delineated by individual ‘luminous’ galaxies (here, with $M_B < -19.0$), or the individual galaxies of pairs and groups (large dots) in Fig. 1. A sample of luminous galaxies, delineating the void, is presented and discussed below. Their lists are given in Tables A1 and A2 in Appendix A.

Constructing this bordering luminous/massive object sample, we first picked up a greater number of luminous objects in the surrounding volume, defined by the sky region with R.A. between 6 h and 11 h and Declinations of $> 0^\circ$ and radial velocities $V_{\text{hel}} < 1800 \text{ km s}^{-1}$, or distances $D \lesssim 30 \text{ Mpc}$. Then, analysing the intermediate results in 3D pictures, we reduced the sample of luminous galaxies in order to leave only those objects which really define the bound-

aries of this void. For galaxies with known non-redshift distances, either from the photometric methods - cepheid, Tip of Red Giant Branch (TRGB), or surface-brightness fluctuations (SBF) or from the Tully-Fisher luminosity-rotation velocity relation (see ‘The Extragalactic Distance Database’, Tully et al. 2009), we computed the ‘distance’ velocity as follows: $V_{\text{dist}} = 73 \times D(\text{Mpc})$.

Tully et al. (2008) noted that galaxies in the region considered here have a large peculiar radial velocity component. This is induced by the giant Local Void being situated approximately on the opposite side of the Local Sheet. The geometry is illustrated in Fig. A1 in the appendix. It shows on a larger scale the position of the Lynx-Cancer void in supergalactic coordinates in two slices, together with both the Local Sheet and the Local Void. The Local Sheet galaxies (including the Local Group), being at the Local Void border, move with $V=323 \text{ km s}^{-1}$ along the vector n , directed to the sky position with coordinates of $l=220^\circ$, $b=32^\circ$ (Tully et al. 2008). To account for this large peculiar velocity, the galaxies for which only redshifts are available require a correction $V_{\text{dist}} = V_{\text{LG}} + V_{\text{pec}}$, where $V_{\text{pec}} = 323 \times (\cos \theta) \text{ km s}^{-1}$ with θ being the angle between the vector n and direction to a galaxy.

To verify the choice of such a correction, we compared the resulting $V_{\text{dist}} = V_{\text{LG}} + V_{\text{pec}}$ for 21 galaxies in the considered region, for which the independent reliable distances are known from TRGB, cepheid or SBF methods. The derived weighted mean difference of $-9 \pm 32 \text{ km s}^{-1}$ is consistent with no systematic difference between the real value and that derived through V_{pec} .

2.3 The Lynx-Cancer void description

Real voids are not perfect spheres. But as the first approximation of a void, we use the largest empty spheres which can be inscribed in the distribution of dots, representing ‘luminous’ galaxies. To find such spheres, we accounted for the borders of the studied volume mentioned in Sec. 2.2. The largest sphere appeared significantly larger and more distant (‘Lynx-Cancer main’ void in Table 1) than that previously suggested in Pustilnik et al. (2003). However, we also identified a smaller sphere, significantly intersecting with the former one (called the Lynx-Cancer subvoid). Its parameters are similar to those of the originally described Lynx-Cancer void from Pustilnik et al. (2003). Both of these spheres are shown in contours in the right-hand panel of Fig. 1. The centre of the main void with radius $R = 8.2 \text{ Mpc}$ is at distance $D = 18.0 \text{ Mpc}$. The centre of the subvoid with $R = 6.0 \text{ Mpc}$ is at $D = 14.6 \text{ Mpc}$.

As described above, in many cases the form of real voids is nonspherical. Also, the modelling of voids (e.g. Lavaux & Wandelt 2010, and references therein) indicates that smaller voids are expected to be more elongated. Therefore, for the subsequent analysis we not only assign to the Lynx-Cancer void region the interior of the two maximal spheres described above, which includes 45 galaxies with $D_{\text{NN}} > 2 \text{ Mpc}$, but also examine galaxies in the adjacent empty regions between the bordering luminous objects and the surfaces of these empty spheres. If these galaxies fall in the regions situated far from luminous galaxies ($D > 2 \text{ Mpc}$), these regions are treated also as parts of the void and the related galaxies are also qualified as void objects. About

half of the dwarf galaxies classified as void objects in Section 3 belong to these empty regions outside the well-defined maximal void spheres.

3 THE DWARF GALAXY SAMPLE WITHIN THE LYNX-CANCER VOID

A sample of 75 dwarf ($-11.9 > M_{\text{B}} > -17.9$) and 4 subluminous [$M_{\text{B}} \sim -(18.0-18.3)$] galaxies, falling within the Lynx-Cancer void, is presented in Table 2. To separate this sample, we proceeded as follows. First, we selected in two steps all isolated galaxies within the void region. At the first step, all galaxies were considered isolated if they had a projected distance to a luminous nearest neighbour $> 1 \text{ Mpc}$. At the second step, for the void galaxies with luminous neighbours closer than 1 Mpc in projection, we used a finer criterion, corresponding to the results on satellites of massive galaxies, presented by Prada et al. (2003).

In the analysis of a very large sample of SDSS galaxies, Prada et al. (2003) have shown that for a galaxy with luminosity L^* , the relative r.m.s. line-of-sight velocities of satellites, σ_{vel} , change from 120 km s^{-1} at 20 kpc to $\sim 80 \text{ km s}^{-1}$ at 200 kpc, and to $\sim 60 \text{ km s}^{-1}$ at 350 kpc. The satellite velocities at large distances scale as $L^{0.5}$ of the host galaxy. To qualify the status of a small galaxy, we took these results into account. Namely, based on the M_{B} and the projected distance of the nearest luminous galaxy, we estimated the respective value of $2\sigma_{\text{vel}}$ following the results of Prada et al. (2003). If $|\Delta V_{\text{rad}}|$ for the small galaxy in question is larger than the estimated $2\sigma_{\text{vel}}$, this dwarf was treated as unrelated to the luminous neighbour, that is as an isolated object. Following Karachentsev (2005), we adopted orbital masses in the range $(2.6 \pm 1.3) \times 10^{12} M_{\odot}$ for groups. According to Prada et al. (2003), this implies values of σ_{vel} of $65-100 \text{ km s}^{-1}$ at $R = 350 \text{ kpc}$, and a factor of 1.5 larger at $R = 100 \text{ kpc}$. Once the isolated galaxies are selected, the distance to the nearest luminous neighbour D_{NN} was then calculated as the length of the 3D radius-vector between the two objects.

Finally, we assign an isolated galaxy to the void galaxy sample if it falls inside the maximal sphere of the main Lynx-Cancer void or its smaller subvoid, as described above, and have $D_{\text{NN}} > 2.0 \text{ Mpc}$. As noted in Section 2.3, we also included in the void sample all isolated galaxies which, due to non-sphericity of the void, appear in the adjacent regions somewhat outside the respective spheres and have $D_{\text{NN}} > 2.0 \text{ Mpc}$.

For two late-type spiral galaxies IC 2233 and NGC 2537, situated on the sky close to each other, we used distances from the detailed study by Matthews & Uson (2008), which finds no evidence or traces of interaction between these two galaxies. A good TRGB distance estimate is known only for the almost edge-on LSB spiral IC 2233. We adopt for this galaxy the mean distance module of three discussed values by Matthews & Uson (2008): $\mu_{\text{mean}} = 30.15 \text{ mag}$, respectively $10.7 \pm 0.5 \text{ Mpc}$. The less accurate NGC 2537 distance estimators are consistent with the galaxies to be unrelated (see Matthews & Uson 2008, for references and detailed discussion). We adopted for the latter galaxy the distance determined from its radial velocity and general peculiar veloc-

ity correction, which appears consistent with the estimates in literature within their accuracies.

In Table 2 we present the following information on galaxies falling into the Lynx-Cancer void.

Column 1. Common name or SDSS prefix.

Columns 2 and 3. Epoch J2000 R.A. and Declination.

Columns 4 and 5. V_{hel} and its error (almost all are either from NED or SDSS). For several objects either without SDSS/NED velocities, or for which this is significantly improved or corrected, we give the latter values. They include PGC2807187 (Karachentsev et al. 2008); pair HS 0822+3542 and SAO 0822+3545, KISSB 23 and SDSS J0926+3343 (Chengalur et al. 2006; Pustilnik & Martin 2007; Pustilnik et al. 2010); UGC 3912 (Springob et al. 2005), SDSS J0723+3621, SDSS J0723+3622, SDSS J0737+4724, SDSS J0852+1351 (Pustilnik et al., MNRAS, submitted), NGC 2537 and IC 2233 (Matthews & Uson 2008).

Column 6. The respective V_{LG} .

Column 7. The velocity V_{dist} (in km s^{-1}) corresponds to $D(\text{Mpc}) \times 73$ when the photometric (TRGB, cepheids) distance estimate $D(\text{Mpc})$ is available (only for 4 galaxies, marked by *, typical accuracy $\sim 10\%$). Otherwise, this is $V_{\text{LG}} + V_{\text{pec}}$, where $V_{\text{pec}} \sim 300 \text{ km s}^{-1}$ is a correction for the peculiar velocity described in Section 2.2. In this case the distance accuracy comes from the quadratic sum of $\sigma(V_{\text{hel}})$ and $\sigma(V_{\text{pec}})$. The first term is $< 10\text{--}15 \text{ km s}^{-1}$ for about 3/4 of all sample galaxies, rising on average to $\sim 30\text{--}40 \text{ km s}^{-1}$ for the rest objects. The second term is 25 km s^{-1} (Tully et al. 2008). Hence, for about 3/4 of the sample galaxies the typical uncertainty $\sigma(V_{\text{dist}})$ is $< 30 \text{ km s}^{-1}$, or $\sigma(D) \lesssim 0.4 \text{ Mpc}$. For the remaining galaxies, the typical $\sigma(V_{\text{dist}})$ is $\sim 40\text{--}45 \text{ km s}^{-1}$, or $\sigma(D) \sim 0.6 \text{ Mpc}$.

Columns 8 and 9. B_{tot} (from NED or from the literature) and the Galaxy extinction A_{B} (from NED, following Schlegel et al. 1998). The sources of B -mag are given by a letter in the superscript for the respective values in the following order. *b*, Karachentsev et al. (2008); *c*, Paturel et al. (2000, 2003); *d*, Barazza et al. (2001); *e*, de Vaucouleurs et al. (1991); *f*, mean of photographic magnitudes from UGC and MCG catalogs, transformed to B -band; *g*, Karachentsev et al. (2001); *h*, Karachentsev et al. (2004); *i*, van Zee (2000); *j*, Garnier et al. (1996); *l*, Matthews & Uson (2008); *m*, Pustilnik et al. (2003); *n*, Pustilnik et al. (2010); *o*, Salzer et al. (2002); *p*, Pustilnik, Kniazev & Pramskij (2005a), *q*, Pustilnik et al., MNRAS, submitted. When B_{tot} was unavailable in the literature, we used the brightest (model) values of the SDSS g and r -filter magnitudes of those presented in NED (if present, or directly from SDSS DR7) and transformed them to B -band magnitudes according to the Lupton et al. (2005) formulae [$B = g + 0.3130(g - r) + 0.2271$; $\sigma = 0.0107$]. This case is marked by superscript *k* after the value of B_{tot} . The resulting rms accuracy σ_{B} for the great majority of the sample galaxies is $\lesssim 0.1\text{--}0.2 \text{ mag}$. However, for several galaxies outside the SDSS zone, for which the CCD photometry appeared unavailable, the σ_{B} can be as large as $\sim 0.5 \text{ mag}$.

Column 10. It presents M_{B} , corrected for A_{B} , calculated from values in Columns 8 and 9 and the distance $D(\text{Mpc})$, corresponding to V_{dist} , that is $D = 73V_{\text{dist}}$.

Column 11. (Tentative) morphological class.

Column 12. The distance in Mpc to the nearest luminous galaxy or group, D_{NN} .

Column 13. Either an alternative name or some important comments, like the presence of companion, etc.

In Figs 2 - 4 we present the mosaic of 64 void galaxy images prepared with the SDSS Navigate Tool. For the remaining 15 void galaxies situated outside the SDSS footprint, we show their images in Fig. 5, as extracted from the combined Palomar Sky Survey O and R images.

4 PROPERTIES OF THE VOID GALAXY SAMPLE AND RELATED ISSUES

4.1 Global properties

The main goal of selecting a galaxy sample falling inside the Lynx-Cancer void is to study evolutionary parameters and to perform a comparison with similar parameters of dwarfs in a more typical and denser environment. The evolutionary parameters can also depend on galaxy global parameters, such as mass or luminosity. Therefore, we present and briefly summarize the distributions of void galaxies with respect to D_{NN} , M_{B} and morphological types. As one can see in the left-hand panel of Fig. 6, about half of the void galaxies have D_{NN} in the range of 2.0–3.5 Mpc, which is close to the adopted threshold value of 2.0 Mpc. This corresponds to the known fact that a large fraction of void galaxies reside close to the void boundaries. Very isolated galaxies, with D_{NN} from 5 to 13 Mpc comprise $\sim 16\%$ of the sample. The blue luminosities of the void galaxies, M_{B} , spread over a range of more than six magnitudes (Fig. 6, right-hand panel), from ~ -12.0 to -18.3 , with the median and peak value of the histogram near ~ -14.5 . The latter indicates the substantial incompleteness of this void sample for $M_{\text{B}} > -14.0$.

A preliminary visual analysis of the void galaxy images in Figs 2–5 shows that about half of them appear Low Surface Brightness (LSB) objects. Two objects are classified as blue compact galaxies (BCGs). These are HS 0822+3542 and HS 1013+3809, both having very low O/H. They both are the components of pairs with more massive galaxies (Kniazev, Pustilnik & Ugryumov 1998; Kniazev et al. 2000; Pustilnik et al. 2003; Kniazev et al. 2003; Pustilnik & Martin 2007). One more galaxy - NGC 2537=Mkn 86 is also classified as a BCG in some works. The remaining objects are either more or less typical late-type dwarf spirals or irregular galaxies with the ‘normal’ level of current SF. More accurate data on the LSB galaxy fraction will be given in a forthcoming paper where the fitting surface brightness (SB) radial profiles is performed and the value of central SB of the underlying discs is estimated.

4.2 Completeness of the void galaxy sample

The study of the luminosity function of void galaxies for absolute magnitudes $M_{\text{B}} \leq -14$ is very important for comparison with the results of CDM cosmological simulations. In particular, the question of how faint and slow-rotating galaxies are found within voids was recently addressed by Tikhonov & Klypin (2009). The latter issue requires a careful analysis of selection effects, which limit the number of

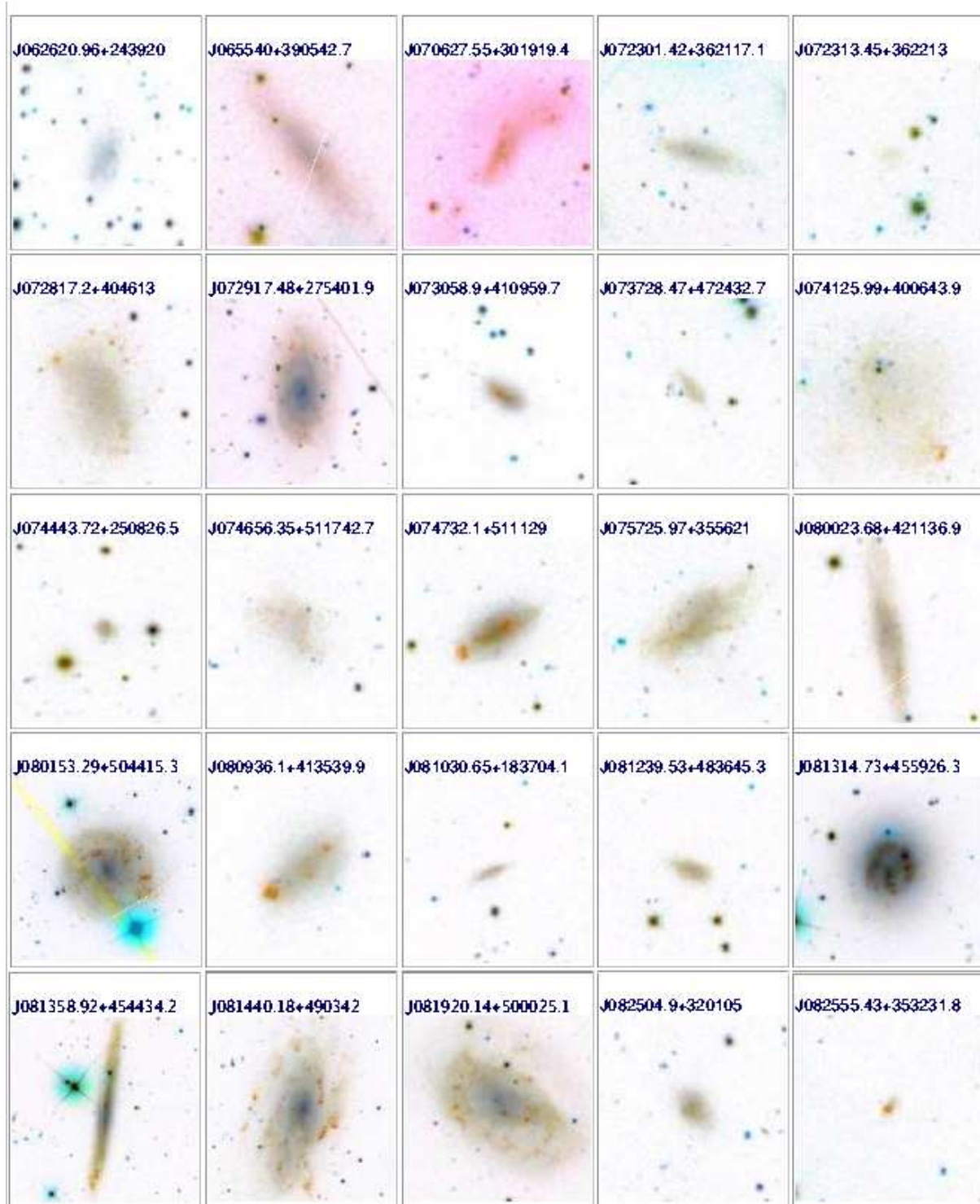


Figure 2. The finding charts of 25 galaxies from the Lynx-Cancer void sample (see Table 2), falling in the zone covered by the SDSS. They are prepared with the SDSS DR7 Navigate Tool with inverted colours and are shown in the order of their RA. The side of each square measures $\approx 100''$, with except of several larger galaxies. For J0729+2754, J0801+5044, J0813+4559 the side is $\approx 200''$, while for J0813+4544, J0814+4903, J0819+5000 the side is $\approx 300''$.

known faint galaxies in the void sample. A better understanding of the spatial structures (filaments) in the void galaxy distribution can also be used as a test of structure formation in low-density regions (Park & Lee 2009).

It is well established that the luminosity and central

SB of galaxies are correlated albeit with rather large scatter. This is shown, in particular, by Cross & Driver (2002), based on bivariate distributions of M_B , $\mu_{B,0}$. The ridge of this bivariate distribution along which $\mu_{B,0}$ systematically changes with M_B is read as

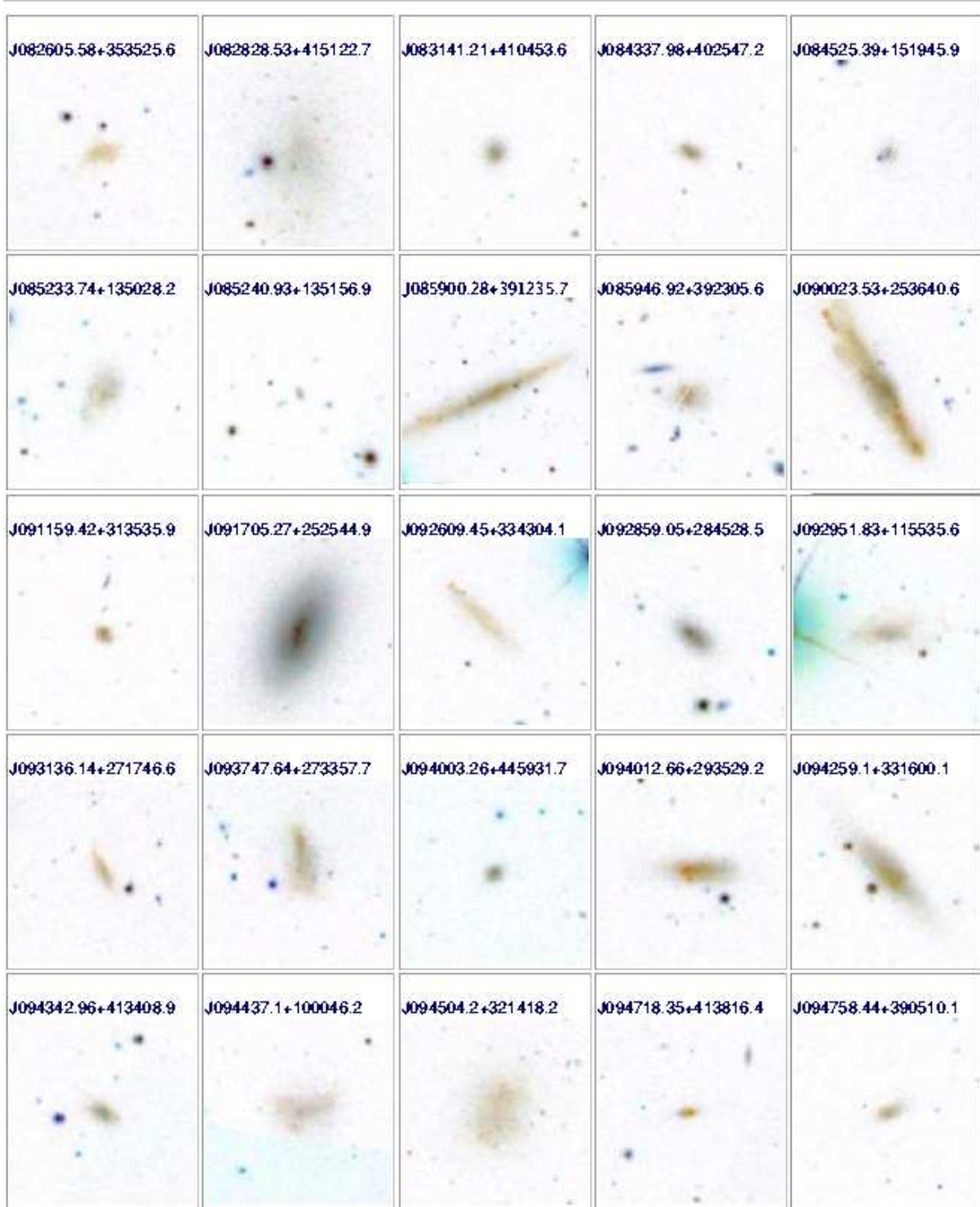


Figure 3. The same as for Fig. 2, for the next 25 galaxies from the Lynx-Cancer void sample, falling in the zone covered by the SDSS. The finding chart size for a larger galaxy J0859+3912 is $\approx 200''$.

$$\mu_{B,0} - \mu_{B,0}^* = \beta_\mu \times (M_B - M_B^*), \quad (1)$$

where $\beta_\mu = 0.281 \pm 0.007$, $\mu_{B,0}^* = 22.65 \text{ mag arcsec}^{-2}$ and $M_B^* = -20.20$. The r.m.s scatter in $\mu_{B,0}$ around this ridge is estimated as $\sigma_\mu = 0.517 \pm 0.006 \text{ mag arcsec}^{-2}$. All the values above were transformed to B -band from the original b_J magnitudes of the 2dFGRS (Two-degree Field Galaxy Red-

shift Survey) in Cross & Driver (2002) using the transform of $B \approx b_J + 0.20 \text{ mag}$. The latter is based on the relation $B = b_J + 0.28(B - V)$ from Hewett et al. (1995) and the typical late-type galaxy colour $(B - V) \sim 0.7$. Using these results, we can address the possible incompleteness of the current Lynx-Cancer void galaxy sample.

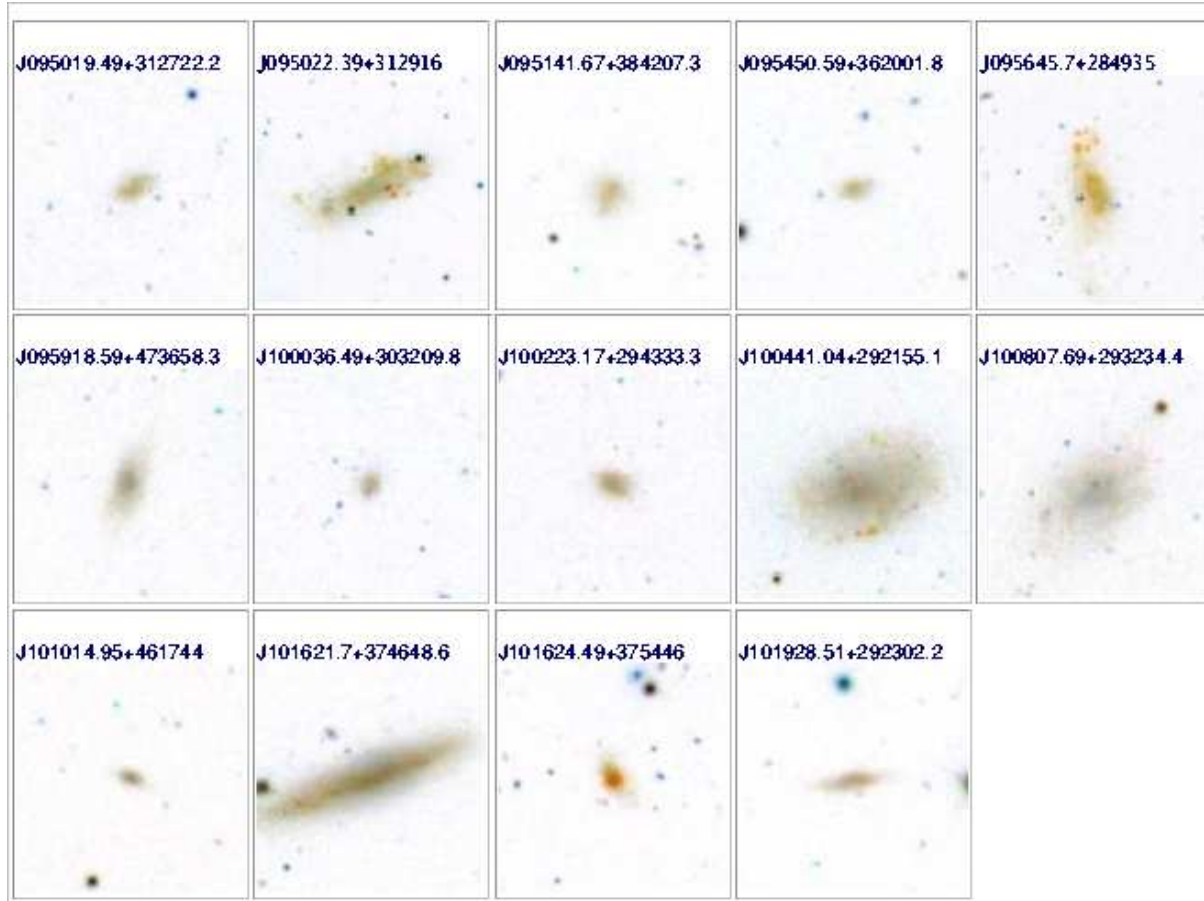


Figure 4. The same as for Fig. 2, for the remaining 14 galaxies from the Lynx-Cancer void sample, falling in the zone covered by the SDSS. The finding chart size of two larger galaxies (J0950+3129, J0956+2849) is $\approx 200''$.

Blanton et al. (2005) and Geha et al. (2006) indicated that the SDSS spectral survey of galaxies is significantly incomplete for the average SB within r -filter half-light radius dimmer than $23.5 \text{ mag arcsec}^{-2}$. We use the effective surface brightness μ_{eff} to derive an estimate of the central SB $\mu_{B,0}$ for comparison with the above study. For this we adopt the colour $g - r \sim 0.5$ as a value typical of late-type dwarfs. We also use the Lupton et al. (2005) formula to convert the SDSS g and r magnitudes to Johnson-Cousins B . For the adopted $(g - r)$ colour, we get a typical value of $B - g \sim 0.35$ and respectively, $B - r \sim 0.85$. From this, $\mu_{\text{eff},r} = 23.5 \text{ mag arcsec}^{-2}$ to first approximation corresponds to $\mu_{\text{eff},B} = 24.35 \text{ mag arcsec}^{-2}$. For purely exponential disks with the scalelength α_E , the radius of the disk including its half-light is equal to $r_{\text{eff}} = 1.678\alpha_E$ (e.g. Impey, Bothum & Malin 1988). Using the definition of μ_{eff} , one can show that for purely exponential disks this parameter is related to the central surface brightness: $\mu_{\text{eff}} = \mu_0 + 1.12$. Thus, the above assertion of Blanton et al. (2005) and Geha et al. (2006) can be formulated as a significant incompleteness of the SDSS spectral targets for late-type dwarfs having the visible central SB (uncorrected for the Galaxy extinction and inclination) $\mu_{0,B} > 23.23 \text{ mag arcsec}^{-2}$.

The latter value of $\mu_{0,B}$, according to the above ridge relation (equation 1), corresponds to an average galaxy with

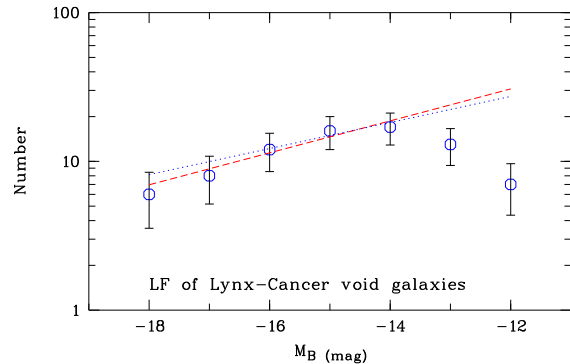


Figure 7. The shape of the raw B -band luminosity function for the Lynx-Cancer void galaxies, fitted by the Schechter functions on the M_B range $[-14.0, -18.0]$. Red dashed line with $\alpha = -1.27 \pm 0.10$ corresponds to the standard $M_B^* = -20.2$ (see text). Blue dotted line with $\alpha = -1.22 \pm 0.09$ corresponds to the ‘reduced’ void value of $M_B^* = -19.2$. The large deficit of galaxies with $M_B \gtrsim -13.5 \text{ mag}$ at least partly is due to the SDSS spectral database selection against LSB galaxies (see text).

$M_B \sim -18.1$. This implies that practically all face-on galaxies (with small contribution of bulge emission) in the void sample are subject to the SDSS spectroscopy SB selection.

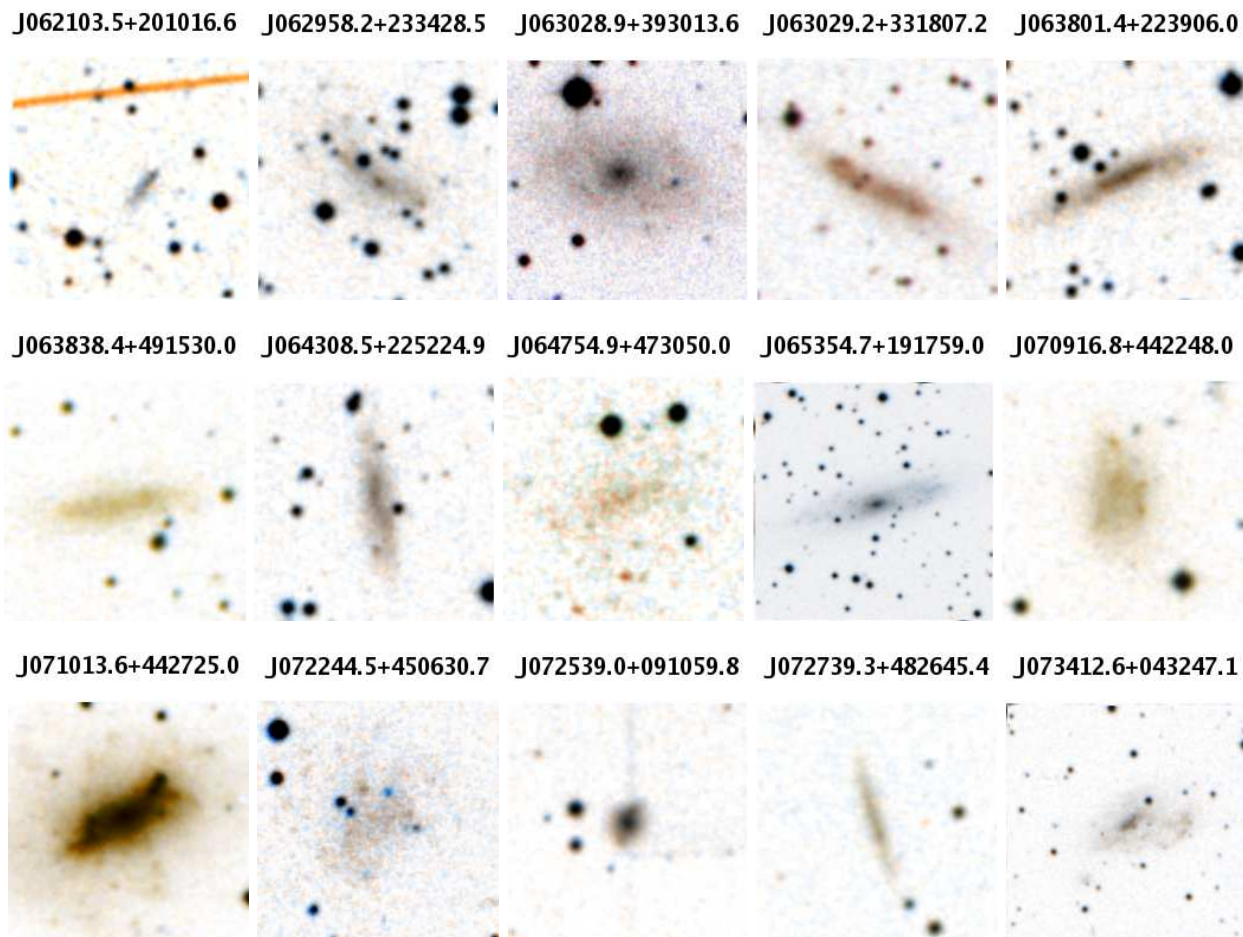


Figure 5. Same as in Fig. 2, but for 15 galaxies from the Lynx-Cancer void sample falling outside the SDSS footprint. They are prepared combining the *O* and *E* images of the Digitized Palomar Sky Survey and are shown in order of their Right Ascension. The colour balance is very approximate. For larger galaxies J0653+1917 and J0743+0432 the size of the chart is $\approx 200''$.

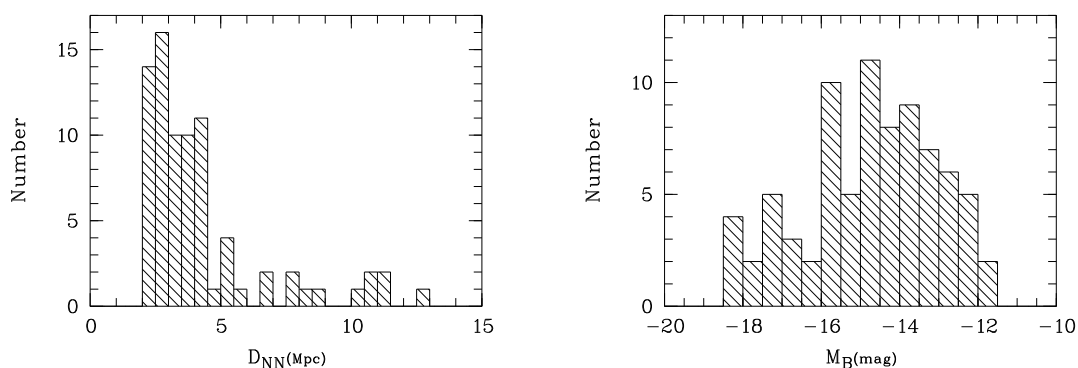


Figure 6. *left panel:* the distribution of distances to the nearest luminous galaxy D_{NN} for the void galaxy sample. *right panel:* the distribution of absolute blue magnitudes M_B for the void galaxies.

The most probable observed inclination angles for the random orientation sample fall around $i=60^\circ$. Therefore, one expects a typical increase of the visible surface brightness of $-2.5 \log(\cos i) \sim 0.75$. The inclination brightening (and the possible presence of central SF regions) thus should mainly eliminate the SDSS SB selection for more luminous void

galaxies. However, it would remain crucial for the fainter void galaxies.

Despite the fact that half of selected Lynx-Cancer void galaxies appear to be LSB galaxies, it is quite evident that LSB dwarfs are under-represented in this sample. This is substantiated by the observation that no

SDSS redshifts could be obtained for several of these LSB dwarfs but are found in the literature as mainly measured via dedicated HI-line observations or through resolved stellar photometry. The examples are LSB dwarfs (LSBDs) UGC 3966 (DDO 46) with HI velocity from Springob et al. (2005), SAO 0822+3545 with H α velocity from Pustilnik et al. (2003), UGC 4426 with photometric distance from Karachentsev et al. (2006), UGC 5209 with HI velocity from Huchtmeier, Karachentsev & Karachentseva (2003).

The effect of the SDSS spectral database magnitude selection for our void sample can be roughly estimated using the adopted Petrosian magnitude limit $r=17.77$. For the great majority of galaxies with sizes less than $1'-2'$, Petrosian magnitudes do not differ more than 0.1 mag from the total galaxy magnitudes. Therefore, using the average colour $(g-r) \sim 0.5$ for late-type galaxies, we transform with the Lupton et al. (2005) formula the limiting value $r=17.77$ to the approximate limiting value $B=18.6$. The distances to the near and distant borders of the Lynx-Cancer void and to its centre, ~ 10 , ~ 26 , and 18 Mpc correspond to distance moduli of $\mu \sim 30.0$, 32.0 and 31.3 mag. This implies, that for the front void ‘hemisphere’, the SDSS should select [if the additional anti-selection of LSB galaxies (LSBGs) would not work] all galaxies with $M_B \lesssim -12.7$, and respectively, for the whole void volume, all galaxies with $M_B \lesssim -13.4$.

In Fig. 7, we show the first approximation of the shape for the void galaxy luminosity function (LF) based on the Table 2 absolute magnitudes. This is fitted by the Schechter function (Schechter 1976) in the range $-14.0 > M_B > -18.0$. Two values of M_B^* are adopted, the standard one of -20.2 mag and the ‘reduced’ one of -19.2 mag, suitable for the void conditions. The LF does not look to be affected by incompleteness down to $M_B \sim -14.0$. The Schechter LF low-luminosity slopes α for these two values of M_B^* are -1.27 ± 0.10 and -1.22 ± 0.09 , respectively. This slope is close to that of the raw LF for the SDSS low-luminosity galaxy sample from Blanton et al. (2005).

According to the ‘ridge’ relation in equation 1, for $M_B = -14.0$ the average value of $\mu_{B,0}$ for disk galaxies corresponds to ~ 24.4 mag arcsec $^{-2}$, that is more than 1 mag arcsec $^{-2}$ dimmer than the derived estimate for the SDSS central surface brightness ‘threshold’. Probably, the significant effect of visible brightening due to galaxy inclination and the presence of central star-forming regions counteracted the SDSS selectivity against LSBGs. However, for galaxies with $-12.0 > M_B \gtrsim -13.5$, our sample could be missing up to 25–30 objects according to the extrapolation of the LF to the lower luminosity range.

There are at least three possible means to find ‘numerous’ missed generic LSB dwarfs within the boundaries of this void. They include: (1) the blind HI surveys (e.g. those mentioned in Section 2.1); (2a) the optical spectroscopy and H α detection of candidate LSB galaxies; and (2b) HI pointing sensitive observations of candidate LSB galaxies. The latter are separated in this sky region from the SDSS image database. Unfortunately, no reliable criteria exist to identify good candidates in the *nearby* LSBDs. Therefore, both methods (2a) and (2b) are not expected to result in a ‘high’ detection rate for galaxies residing in the nearby voids. However, all new redshifts of LSBDs will advance our understanding of the dwarf galaxy census in the local Universe.

4.3 Other properties of, and the prospects of studying, the void sample galaxies

The whole set of the studied sample galaxies includes 75 dwarfs. Observations and the subsequent analysis of this full dataset and comparison with similar data on the control dwarf galaxy sample in a denser environment will require a significant effort during coming years. However, the data collected so far already suggest differences in the evolutionary status of some Lynx-Cancer void dwarf galaxies and those in denser surroundings. While selection effects might play a role, it is unlikely to influence the resulting parameters of the discovered unevolved void dwarf galaxies discussed below.

To examine possible differences in the evolutionary status of void galaxies, we study the following parameters. The first is the gas metallicity as traced by O/H in HII regions around the sites of star formation. The second parameter, the gas mass-fraction, defined as the ratio $M(\text{gas})/M_{\text{bary}}$, where $M_{\text{bary}} = M(\text{HI} + \text{He}) + M_{\text{star}}$. The contribution of molecular gas in the total gas mass of dwarf galaxies is small. While the parameter $M(\text{HI} + \text{He})$ is well determined directly from the HI 21-cm line flux and the adopted ratio $n(\text{He})/n(\text{HI})$, the parameter M_{star} is a more model-dependent. However, with good surface photometry in several filters, like that extracted from the SDSS images and the adopted stellar metallicity, it can be well estimated within reasonable assumptions using popular models like PEGASE (Fioc & Rocca-Volmerange 1999). The third parameter related to the evolutionary status of a galaxy is the age of its the oldest resolved or also unresolved visible stars. The former is hard to obtain and would require long observations even with the Hubble Space Telescope or similar telescopes, even for the fairly local Lynx-Cancer void galaxies. The ground-based surface photometry can be a reasonable alternative. However, the age estimate require well-resolved multicolour deep galaxy images as well as accounting for the potential contamination of nebular emission (if present) and corrections for the dust extinction. Again, the SDSS images of well resolved galaxies and the PEGASE package models are quite often suitable for estimates of this parameter. Examples of such an analysis for two very metal-poor Lynx-Cancer void galaxies, DDO 68 and SDSS J0926+3343, are published by Pustilnik et al. (2008, 2010).

It is worth mentioning that a significant fraction of the void galaxies are paired with typical projected distances in pairs of several tens of kpc. These include the following Lynx-Cancer void list entries: (13,14), (16,17), (27,28), (40,41), (46,47), (66,67), (77,78). Other galaxies look like they are forming unbound but probably coherent elongated structures (‘filaments’) with total length of ~ 1 –2 Mpc. Examples are the chains of entries: (13,14,15,24), (53,60,63,66,67), (59,70,74). The majority of the void galaxies at the current level of its census appear, however, quite isolated.

As mentioned in Section 2.1, several unusual and/or very metal-poor dwarf galaxies fall in the Lynx-Cancer void volume. These include a very low-metallicity BCG HS 0822+3542 [$12 + \log(\text{O}/\text{H}) = 7.44$] and its companion, very blue (and presumably relatively young) LSB dwarf SAO 0822+3545 (Pustilnik et al. 2003). The two most metal-poor dwarf galaxies in the Local Volume and adjacent regions, DDO 68 and SDSS J0926+3343, with the parameters

$12+\log(\text{O}/\text{H})$ of 7.14 and 7.12, respectively, are representatives of this void galaxy population. Moreover, they are situated only at 1.6 Mpc from each other. Both of them are also unusual in the blue colours of their outer parts, indicating ages of the oldest visible stellar population of $\lesssim 1-3$ Gyr (Pustilnik et al. 2008, 2010), which is in drastic contrast with the colours and ages of the absolute majority of other dwarf galaxies. At least three other Lynx-Cancer void dwarf galaxies have $12+\log(\text{O}/\text{H}) \lesssim 7.3$. They include SDSS J0812+4836 (Izotov & Thuan 2007) and SDSS J0737+4724, SDSS J0852+1350, and one more blue 'young' dwarf SDSS J0723+3622 (Pustilnik et al., MNRAS, submitted).

The Lynx-Cancer void interior represents a small fraction (<0.05) of the whole volume to the distance $D = 26$ Mpc. The existence in this void of the concentration of extremely metal-poor galaxies and objects that lack visible old stellar populations is surprising. The former fact is indicative of the physical relationship between the evolutionary status of low-mass late-type galaxies and their global environment. In turn, the latter fact hints at the possibility of retarded galaxy formation in the void environment.

5 SUMMARY

(i) The nearby Lynx-Cancer void is described as a low-density region bordering the Local Volume at negative supergalactic Z coordinates, with the overall extent of more than 16 Mpc and distance to the void centre of 18 Mpc. A smaller subvoid is identified with the centre position on distance of 14.6 Mpc and radius of 6.0 Mpc (close to that described in Pustilnik et al. 2003).

(ii) A sample of 75 late-type dwarf and four subluminal galaxies residing in the void region is presented. Their main observational parameters available in the literature are collected for further study and comparison.

(iii) The shape of the Lynx-Cancer void galaxy raw LF indicates a significant drop in the galaxy number at absolute magnitudes $M_B \gtrsim -14$. This is probably related to the SDSS galaxy spectral database selectivity against LSB galaxies. To remedy this drawback, we mention three possible methods.

(iv) Properties of several unusual dwarf galaxies found to date in the Lynx-Cancer void are briefly described, with the emphasis on their very low metallicities and relatively small ages of the oldest visible stellar populations. These data, despite being rather limited, suggest that the void-type environment might effectively slow down the rate of evolution of a fraction of low-mass galaxies and postpone their formation epoch.

ACKNOWLEDGEMENTS

We thank the anonymous referee for suggestions and criticism which helped to significantly improve the quality and clarity of the data presentation and discussion. We are thankful to D.I. Makarov for providing the list of groups prior publication and A.Y. Kniazev for useful comments on the manuscript. This work was supported through the RFBR grants No. 06-02-16617 to SAP and ALT and No. 10-02-92650 to SAP. SAP is also grateful for the support through the Russian Federal Agency of Education grant No.

2.1.1/1937. We acknowledge the spectral and photometric data used for this study and the related information available in the SDSS database. The Sloan Digital Sky Survey (SDSS) is a joint project of the University of Chicago, Fermilab, the Institute for Advanced Study, the Japan Participation Group, the Johns Hopkins University, the Max-Planck-Institute for Astronomy (MPIA), the Max-Planck-Institute for Astrophysics (MPA), New Mexico State University, Princeton University, the United States Naval Observatory, and the University of Washington. Apache Point Observatory, site of the SDSS telescopes, is operated by the Astrophysical Research Consortium (ARC). This research has made use of the NASA/IPAC Extragalactic Database (NED), which is operated by the Jet Propulsion Laboratory, California Institute of Technology, under contract with the National Aeronautics and Space Administration. We also acknowledge the usage of the HyperLeda database (<http://leda.univ-lyon1.fr>).

REFERENCES

- Abazajian K.N., Adelman-McCarthy J.K., Agüeros M.A., et al., 2009, *ApJS*, 182, 543
 Arkhipova N.A., Komberg B.V., Lukash V.N., Mikheeva E.V., 2007, *Astr.Rep.* 51, 787
 Barazza F.D., Binggeli B., Prugniel P., 2001, *A&A*, 373, 12
 Begum A., Chengalur J.N., Karachentsev I.D., Sharina M.E., Kaisin S.S., 2008, *MNRAS*, 386, 1667
 Blanton M.B., Lupton R., Schlegel D.J., Strauss M.A., Brinkmann J., Fukugita M., Loveday J., 2005, *ApJ*, 631, 208
 Boselli A., Gavazzi G., 2006, *PASP*, 118, 517
 Chengalur J.N., Pustilnik S.A., Martin J.-M., Kniazev A.Y., 2006, *MNRAS*, 371, 1849
 Cross N., Driver S.P., 2002, *MNRAS*, 329, 579
 de Vaucouleurs G., de Vaucouleurs A., Corwin H.G., Buta R.J., Paturel G., Fouqué P., 1991, *Third Reference Catalog of Bright Galaxies*, version RC3.9
 Fairall A., 1998, *Large-Scale Structures in the Universe*, Wiley-Praxis, 196 pp.
 Fioc M. & Rocca-Volmerange B., 1999, *arXiv:astro-ph/9912179*
 Fukugita M., Ichikawa T., Gunn J.E., et al. 1996, *AJ*, 111, 1748
 Garnier R., Paturel G., Petit C., Marthinet M.C., Rousseau J., 1996, *A&AS*, 117, 467
 Geha M., Blanton M.R., Masjedi M., West A.A., 2006, *ApJ*, 653, 240
 Gottlöber S., Lokas E.L., Klypin A., Hoffman Y., 2003, *MNRAS*, 344, 715
 Gunn J.E., Carr M.A., Rockosi C.M. et al., 1998, *AJ*, 116, 3040
 Hahn O., Carollo C.M., Porciani C., Dekel A., 2007, *MNRAS*, 381, 41
 Hahn O., Porciani C., Dekel A., Carollo C.M., 2009, *MNRAS*, 398, 1724
 Haynes M., 2008, *Dark Galaxies and Lost Baryons*, Proc. of IAU Symposium, ed. by J.I. Davies & M.J. Disney, Vol. 244, p. 83, Cambridge Univ. Press.

- Haynes M.P., Giovanelli R., & Chincarini G.L., 1984, *ARA&A*, 22, 445
- Hewett P.C., Foltz C.B., Chaffee F.H., 1995, *AJ*, 109, 1498
- Hoefl M., Yepes G., Gottlöber S., Springel V., 2006, *MNRAS*, 371, 401
- Huchtmeier W.K., Karachentsev I.D., Karachentseva V.E., 2003, *A&A*, 401, 483
- Impey C., Bothun G., Malin D., 1988, *ApJ*, 330, 634
- Izotov Y.I., Thuan T.X., 2007, *ApJ*, 665, 1115
- Johnston S., Taylor B., Bailes M., et al. 2008, *Experimental Astronomy*, 22, 151
- Karachentsev I.D., 2005, *AJ*, 129, 178
- Karachentsev I.D., Makarov D.I., 2008, *Astrophys.Bull.*, 63, 299
- Karachentsev I.D., Karachentseva V.E., Huchtmeier W.K., 2001, *A&A*, 366, 482
- Karachentsev I.D., Karachentseva V.E., Huchtmeier W.K., Makarov D.I., 2004, *AJ*, 127, 2031
- Karachentsev I.D., Dolphin A., Tully R.B., et al. 2006, *AJ*, 131, 1361
- Karachentsev I.D., Makarov D.I., Karachentseva V.E., Melnik O.V., 2008, *Astronomy Letters*, 34, 832
- Kniazev, A.Y., Pustilnik, S.A., Ugryumov, A.V. 1998, *Bulletin SAO*, 46, 23
- Kniazev, A.Y., Pustilnik, S.A., Masegosa, J., et al., 2000, *A&A*, 357, 101
- Kniazev, A.Y., Grebel, E.K., Hao L., Strauss M., Brinkmann J., Fukugita M., 2003, *ApJ*, 593, L73
- Lavaux G., Wandelt B.D., 2010, *MNRAS*, 403, 1392
- Lindner U., Einasto J., Einasto M., et al., 1996, *A&A*, 314, 1
- Lupton R., et al. 2005, <http://www.sdss.org/dr5/algorithms/sdssColorTransformations.html>, Chapter 205
- Makarov D.I., Karachentsev I.D., 2009, *Astrophys. Bull.*, 64, 24
- Makarov D.I., Karachentsev I.D., 2011, *MNRAS*, 412, 2498
- Mathis H., White S.D.M., 2002, *MNRAS*, 337, 1193
- Matthews L.D., Uson J.M., 2008, *AJ*, 135, 291
- Oosterloo T., Verheijen M., van Cappelen W., 2010, *Proc. of the ISKAF2010 Science Meeting*. June 10 -14 2010. Assen, the Netherlands. PoS, ISKAF2010, 043
- Park D., Lee J., 2009, *MNRAS*, 397, 2163
- Patiri S.G., Prada F., Holtzman J., Klypin A., Betancort-Rijo J., 2006, *MNRAS*, 372, 1710
- Paturel G., Fang Y., Garnier R., Petit C., Rousseau J., 2000, *A&A Suppl. Ser.*, 146, 19
- Paturel G., Petit C., Prugniel P., Theureau G., Rousseau J., Brouty M., Dubois P., Cambrésy L., 2003, *A&A*, 412, 45
- Peebles P.J.E., 2001, *ApJ*, 557, 459
- Pier J.R., Munn J.A., Hindsley R.B. et al., 2003, *AJ*, 125, 1559
- Popescu C.C., Hopp U., Elsässer H., 1997, *A&A*, 325, 881
- Prada F., Vitvitska M., Klypin A., et al., 2003, *ApJ*, 598, 260
- Pustilnik S.A., Martin J.-M., 2007, *A&A*, 464, 859
- Pustilnik S.A., Ugryumov A.V., Lipovetsky V.A., Thuan T.X., Guseva N.G., 1995, *ApJ*, 443, 499
- Pustilnik S.A., Martin J.-M., Huchtmeier W., Brosch N., Lipovetsky V.A., 2002, *A&A*, 389, 405
- Pustilnik S.A., Kniazev A.Y., Pramsky A.G., Ugryumov A.V., Masegosa J., 2003, *A&A*, 409, 917
- Pustilnik S.A., Kniazev A.Y., Pramsky A.G., Izotov Y.I., Foltz C., Brosch N., Martin J.-M., Ugryumov A., 2004, *A&A*, 419, 469
- Pustilnik S.A., Kniazev A.Y., Pramskij A.G., 2005, *A&A*, 443, 91
- Pustilnik S.A., Engels D., Lipovetsky V.A., et al., 2005, *A&A*, 442, 109
- Pustilnik S.A., Engels D., Kniazev A.Y., Pramskij A.G., Ugryumov A.V., Hagen H.-J., 2006, *Astron.Lett.* 32, 228
- Pustilnik S.A., Tepliakova A.L., Kniazev A.Y., 2008, *Astron.Lett.*, 34, 457 (arXiv:0712.4007)
- Pustilnik S.A., Tepliakova A.L., Kniazev A.Y., Burenkov A.N., 2010, *MNRAS*, 401, 333
- Rojas R.R., Vogeley M.S., Hoyle F., Brinkmann J., 2004, *ApJ*, 617, 50
- Rojas R.R., Vogeley M.S., Hoyle F., Brinkmann J., 2005, *ApJ*, 624, 571
- Salzer J.J., 1989, *ApJ*, 347, 152
- Salzer J.J., Gronwall C., Sarajedini V.L. 2002, *AJ*, 123, 1292
- Schechter P., 1976, *ApJ*, 203, 297
- Schlegel D.J., Finkbeiner D.P., Douglas M. 1998, *ApJ*, 500, 525
- Schneider S.E., Thuan T.X., Magri C., Wadiak J.E., 1990, *ApJS*, 72, 245
- Smith J.A., Tucker D.L., Kent S. et al., 2002, *AJ*, 123, 2121
- Sorrentino G., Antonuccio-Delogu V., Rifatto A., 2006, *A&A*, 460, 673
- Springob C.M., Haynes M.P., Giovanelli R., Kent B.R., 2005, *ApJS*, 160, 149
- Stanonik K., Platen E., Aragón-Calvo M.A., et al., *Galaxies in Isolation: Exploring Nature Versus Nurture*, proceedings of the IAU Symposium #249, held 2005 to 15 May 2009 in Granada, Spain. Edited by Lourdes Verdes-Montenegro, Ascension del Olmo, and Jack Sulentic. San Francisco: Astronomical Society of the Pacific, 2010, p.107
- Tikhonov A.V., Klypin A.A., 2009, *MNRAS*, 395, 1915
- Tully R.B., Somerville R.S., Trentham N., Verheijen M.A.W., 2002, *ApJ*, 569, 573
- Tully R.B., Shaya E.J., Karachentsev I.D., Courtois H.M., Kocevski D.D., Rizzi L., Peel A., 2008, *ApJ*, 676, 184
- Tully R.B., Rizzi L., Shaya E.J., Courtois H.M., Makarov D.I., Jacobs B.A., 2009, *AJ*, 138, 323
- van de Weygaert R., Platen E., Tigrak E., Hidding J., van der Hulst J.M., Aragón-Calvo M.A., Stanonik K., van Gorkom J.H., 2009, in *ASP Conf.Ser.*, 421, 99
- van Zee L., 2000, *AJ*, 119, 2757
- Ugryumov A.V., Engels D., Lipovetsky V.A., et al., 1999, *A&AS*, 135, 511
- Winkel B., Kalberla P.M.W., Kerp J., Flöer L., 2010, *ApJS*, 188, 408
- York D.G., Adelman J., Anderson J.E. et al. 2000, *AJ*, 120, 1579

Table 2. Main parameters of dwarf galaxies inside the Lynx-Cancer void

#	Name or prefix (1)	Coordinates (J2000) (2) (3)		V_{hel} (4)	σ_V (5)	V_{LG} (6)	V_{dist} (7)	B_{tot} (8)	A_B (9)	M_B (10)	Type (11)	D_{NN} (12)	Other names and notes (13)
1	PGC2807187	06 21 03.51	+20 10 16.6	1318	7	1263	1513	18.00 ^b	3.63	-17.21	Scd	12.76	ADBS J062103+2010
2	HIPASSJ0626+24	06 26 20.97	+24 39 20.0	1473	7	1432	1682	17.60 ^b	1.79	-16.0	Scd	11.39	
3	PGC1689759	06 29 58.23	+23 34 28.5	1452	6	1426	1680	17.10 ^b	1.18	-15.89	Scd	11.36	
4	UGC3475	06 30 28.86	+39 30 13.6	487	1	524	752	14.97 ^c	0.79	-15.88	Sm	5.11	MCG 7-14-2
5	UGC3476	06 30 29.22	+33 18 07.2	469	4	477	718	14.96 ^d	1.02	-16.02	Im	4.89	CGCG 175-2
6	UGC3503	06 38 01.40	+22 39 06.0	1389	4	1347	1608	15.10 ^e	0.66	-17.27	Sd	10.96	
7	UGC3501	06 38 38.40	+49 15 30.0	449	6	528	735	17.20 ^f	0.50	-13.31	Im	4.24	MCG 8-12-031
8	UGC3516	06 43 08.51	+22 52 24.9	1287	7	1226	1491	16.97 ^c	1.19	-15.79	Sd	10.78	
9	KKH 38	06 47 54.88	+47 30 50.0	451	2	518	725	17.40 ^g	0.40	-12.99	Ir	4.31	LEDA 2807122
10	UGC3587	06 53 54.70	+19 17 59.0	1267	1	1194	1470	13.84 ^e	0.40	-18.08	S?	10.47	
11	UGC3600	06 55 40.00	+39 05 42.8	412	4	435	679	16.18 ^h	0.29	-13.95	Im	3.85	PGC 019871
12	UGC3672	07 06 27.56	+30 19 19.4	994	4	968	1236	15.40 ⁱ	0.32	-16.08	Im	8.54	PGC 20154
13	UGC3698	07 09 16.80	+44 22 48.0	422	1	465	701	15.41 ^h	0.42	-14.92	Im	3.82	Pair with NGC 2337
14	NGC2337	07 10 13.60	+44 27 25.0	436	1	479	715	13.48 ^h	0.38	-16.85	IBm	3.91	Pair with UGC 3698
15	UGC3817	07 22 44.48	+45 06 30.7	437	1	478	717	15.96 ^h	0.44	-14.44	Im	3.71	PGC 20852
16	SDSS	07 23 01.42	+36 21 17.1	885	3	882	1050	17.01 ^q	0.23	-14.19	Sm?	6.55	
17	SDSS	07 23 13.46	+36 22 13.0	974	3	971	1050	19.25 ^q	0.23	-11.95	dI	6.55	Companion? of J0723+3621
18	PGC020981	07 25 38.95	+09 10 59.8	1202	6	1064	1363	16.69 ^c	0.27	-14.94	I	8.18	CGCG 057-013
19	UGC3853	07 27 39.26	+48 26 45.4	936	4	992	1231	15.96 ^j	0.46	-15.65	Sdm	4.20	MCG 8-14-018=RFGC 1217
20	UGC3860	07 28 17.20	+40 46 13.0	354	1	371	570*	14.96 ^e	0.25	-14.75	Im	2.51	DDO 43
21	UGC3876	07 29 17.49	+27 54 01.9	854	6	806	1096	13.70 ^e	0.19	-17.39	SAd	7.81	MCG 5-18-15=KARA 193
22	SDSS	07 30 58.90	+41 09 59.8	874	3	892	1146	16.67 ^k	0.27	-14.58	dI	5.25	SDSS J073058.90+410959.8
23	UGC3912	07 34 12.63	+04 32 47.1	1240	5	1065	1368	14.72 ^c	0.23	-16.87	S?	7.62	
24	SDSS	07 37 28.47	+47 24 32.8	476	2	524	761	18.06 ^q	0.47	-12.50	LSB	3.22	SDSS J073728.49+472432.8
25	UGC3966	07 41 26.00	+40 06 44.0	361	5	370	631	14.44 ^c	0.22	-15.46	Im	2.37	DDO 46
26	SDSS	07 44 43.72	+25 08 26.6	749	4	680	945	18.35 ^k	0.18	-12.39	Ir	5.82	SDSS J074443.72+250826.6
27	MCG9-13-52	07 46 56.36	+51 17 42.8	445	2	510	737	16.78 ^k	0.27	-13.51	Sm	3.02	KKH 40; Comp. of MCG9-13-56
28	MCG9-13-56	07 47 32.10	+51 11 29.0	439	3	503	730	15.48 ^k	0.30	-14.90	Sm	2.93	CGCG 262-28=KUG 0743+513
29	UGC4117	07 57 25.98	+35 56 21.0	773	1	754	1031	15.34 ⁱ	0.20	-15.61	IBm	5.24	MCG 6-18-3=KUG 0754+360
30	UGC4148	08 00 23.68	+42 11 37.0	716	3	729	989	15.63 ^c	0.18	-15.21	Scd	3.73	MCG 7-17-6=KUG0756+423
31	NGC2500	08 01 53.30	+50 44 15.4	504	1	562	794	12.23 ^c	0.17	-18.13	SBcd	2.27	UGC4165=KARA 224
32	MCG7-17-19	08 09 36.10	+41 35 40.0	704	1	712	976	16.65 ^c	0.22	-14.20	Sc	3.76	KUG 0806+417
33	SDSS	08 10 30.65	+18 37 04.1	1483	3	1371	1683	18.29 ^k	0.16	-13.68	Sm:	4.39	
34	SDSS	08 12 39.53	+48 36 45.4	521	5	565	807	17.23 ^k	0.22	-13.21	dIr	2.50	SDSS J081239.53+483645.4
35	NGC2537	08 13 14.73	+45 59 26.3	445	1	475	720	12.27 ^c	0.23	-17.93	SBm	2.95	UGC4274, not pair of IC2233
36	IC2233	08 13 58.93	+45 44 34.3	553	1	572	781*	13.05 ^l	0.22	-17.32	Sd	3.04	UGC4278=RFGC 1340
37	NGC2541	08 14 40.18	+49 03 42.1	548	1	594	876*	12.25 ^c	0.22	-18.36	SABc	2.33	UGC4284, pair with NGC2552?
38	NGC2552	08 19 20.14	+50 00 25.2	524	1	574	811	12.92 ⁱ	0.20	-17.51	SAm	2.24	UGC4325 pair with NGC2541?
39	KUG 0821+321	08 25 04.90	+32 01 05.1	648	16	601	894	16.10 ^k	0.20	-14.54	Ir	4.41	SDSS J082504.94+320105.1
40	HS 0822+3542	08 25 55.43	+35 32 31.9	720	2	691	985	17.92 ^m	0.20	-12.93	BCG	4.46	Pair with SAO 0822+3545
41	SAO0822+3545	08 26 05.59	+35 35 25.7	740	1	711	985	17.56 ^m	0.20	-13.29	Im	4.45	Pair with HS 0822+3542

* V_{dist} calculated from photometric distance.

Table 2. Main parameters of dwarf galaxies inside the Lynx-Cancer void. Continued

#	Name or prefix (1)	Coordinates (J2000) (2) (3)		V_{hel} (4)	σ_V (5)	V_{LG} (6)	V_{dist} (7)	B_{tot} (8)	A_B (9)	M_B (10)	Type (11)	D_{NN} (12)	Notes (13)
42	UGC4426	08 28 28.53	+41 51 22.8	397	4	402	752*	15.13 ^c	0.16	-15.09	Im	2.66	DDO 52
43	SDSS	08 31 41.21	+41 04 53.7	582	40	581	850	17.71 ^k	0.16	-12.78	LSB	3.70	SDSS J083141.21+410453.9
44	SDSS	08 43 37.98	+40 25 47.2	614	3	608	880	17.83 ^k	0.14	-12.72	Im	3.49	SDSS J084337.98+402547.2
45	SDSS	08 45 25.40	+15 19 46.0	1642	50	1504	1824	18.60 ^k	0.09	-13.48	dI	5.11	
46	SDSS	08 52 33.75	+13 50 28.3	1511	4	1364	1685	17.43 ^g	0.16	-14.55	Im	4.05	
47	SDSS	08 52 40.94	+13 51 56.9	1541	22	1394	1685	19.73 ^g	0.16	-12.25	dI	4.05	companion of J0852+1350
48	UGC4704	08 59 00.28	+39 12 35.7	596	6	581	857	15.51 ^c	0.13	-14.97	Sdm	3.20	MCG 7-19-11=KUG0855+394
49	SDSS	08 59 46.93	+39 23 05.6	588	34	573	849	16.98 ^k	0.11	-13.46	dI	3.16	companion of UGC4704
50	UGC4722	09 00 23.54	+25 36 40.6	1794	7	1728	2036	15.16 ^k	0.17	-17.24	Sdm	4.13	merger?
51	SDSS	09 11 59.43	+31 35 35.9	750	4	692	987	17.97 ^k	0.07	-12.75	dI	3.90	SDSS J091159.43+313535.9
52	IC2450	09 17 05.27	+25 25 44.9	1644	2	1552	1859	13.84 ^e	0.14	-18.33	S0:	4.09	UGC 4902=MRK 1230
53	SDSS	09 26 09.45	+33 43 04.1	536	2	488	776	17.34 ^p	0.08	-12.90	LSB	2.89	SDSS J092609.45+334304.1
54	SDSS	09 28 59.06	+28 45 28.5	1229	41	1154	1453	16.70 ^k	0.09	-14.88	dI	2.50	
55	SDSS	09 29 51.83	+11 55 35.7	1614	51	1454	1773	17.36 ^k	0.11	-14.69	dI	2.25	
56	SDSS	09 31 36.15	+27 17 46.6	1505	2	1422	1723	17.98 ^k	0.08	-13.96	Sm?	2.34	
57	KUG0934+277	09 37 47.65	+27 33 57.7	1594	2	1538	1837	16.53 ^k	0.08	-15.55	Im	3.23	KKH 52, in KUG classif. as GPair
58	SDSS	09 40 03.27	+44 59 31.7	1246	80	1260	1512	17.96 ^k	0.06	-13.69	dI	3.99	
59	KISSB23	09 40 12.67	+29 35 29.3	505	2	450	745	16.32 ^o	0.10	-13.82	Sd	2.23	KUG 0937+298
60	UGC5186	09 42 59.10	+33 16 00.2	551	1	501	786	16.27 ^h	0.06	-13.95	Im	2.58	KUG 0940+334
61	SDSS	09 43 42.97	+41 34 08.9	1403	40	1398	1662	17.63 ^k	0.06	-14.22	dI	2.11	
62	SDSS	09 44 37.11	+10 00 46.3	1477	66	1307	1622	16.95 ^k	0.12	-14.90	dI	2.12	
63	UGC5209	09 45 04.20	+32 14 18.2	538	1	482	770	16.06 ^h	0.08	-14.14	Im	2.75	KKH 54
64	SDSS	09 47 18.35	+41 38 16.4	1389	2	1384	1647	17.61 ^k	0.07	-14.22	dI	2.64	
65	SDSS	09 47 58.45	+39 05 10.1	1479	62	1460	1730	18.12 ^k	0.07	-13.82	dI	2.17	
66	UGC5272b	09 50 19.49	+31 27 22.3	539	4	483	750	17.68 ^h	0.10	-12.48	Im	2.51	KK 78, companion of UGC5272
67	UGC5272	09 50 22.40	+31 29 16.0	520	5	464	752	14.46 ^c	0.10	-15.70	Im	2.50	DDO 64=MCG 5-23-41
68	SDSS	09 51 41.67	+38 42 07.3	1435	4	1414	1684	17.42 ^k	0.08	-14.47	dI	2.62	
69	SDSS	09 54 50.60	+36 20 01.9	503	55	470	746	17.93 ^k	0.04	-12.16	dI	2.39	
70	UGC5340	09 56 45.70	+28 49 35.0	502	5	428	720	14.60 ^p	0.08	-15.45	BC/Im	2.06	DDO 68=MCG 5-24-4=VV542
71	PC0956+4751	09 59 18.60	+47 36 58.4	1093	4	1122	1362	17.14 ^k	0.07	-14.28	dI	2.77	SDSS J095918.68+473658.5
72	SDSS	10 00 36.50	+30 32 09.8	501	37	436	723	18.06 ^k	0.08	-12.00	dI	2.17	SDSS J100036.54+303209.8
73	KUG0959+299	10 02 23.18	+29 43 33.3	766	45	697	984	17.32 ^k	0.10	-13.43	dI	2.98	
74	UGC5427	10 04 41.05	+29 21 55.2	498	5	427	715	14.89 ^h	0.10	-15.16	SABd	2.02	MCG 5-24-10
75	UGC5464	10 08 07.70	+29 32 34.4	1003	3	948	1234	15.62 ^e	0.10	-15.62	Sm	3.70	DDO 72=MCG 5-24-17
76	SDSS	10 10 14.96	+46 17 44.1	1092	3	1114	1356	18.20 ^k	0.03	-13.17	dI	3.23	SDSS J101014.96+461744.1
77	UGC5540	10 16 21.70	+37 46 48.7	1162	4	1134	1399	14.60 ^e	0.07	-16.89	Sc	3.21	Pair with HS 1013+3809
78	HS 1013+3809	10 16 24.50	+37 54 46.0	1173	3	1145	1409	15.99 ^k	0.07	-15.51	BCG	3.22	KUG 1013+381, pair with UGC5540
79	SDSS	10 19 28.52	+29 23 02.3	874	43	831	1113	17.43 ^k	0.14	-13.63	dI	2.67	

APPENDIX A: LISTS OF GALAXIES DELINEATING THE LYNX-CANCER VOID

In Tables A1 and A2, we summarize the parameters of objects delineating the Lynx-Cancer void, which include, respectively, 10 ‘isolated’ luminous galaxies and 34 pairs and groups hosting of luminous galaxies. The following information is presented in columns of Table A1. Column 1 - the galaxy name. Columns 2 and 3 - J2000 R.A. and Declination, respectively. Columns 4 and 5 - heliocentric velocity and its error (as extracted from NED). Columns 6 and 7 - the velocity relative to the LG centre and the adopted ‘distance’ velocity ($D(\text{Mpc})=V_{\text{dist}}/73$). Columns 8 and 9 - the total blue magnitude and the adopted B -band the Galaxy extinction correction for the absolute blue magnitude in column 10. In column 11 the ‘NED based’ galaxy morphological type is shown. In column 12, the distance in Mpc to the nearest luminous galaxy is presented. In column 13, some alternative galaxy names are given. Three galaxies with formal $M_B > -19.0$ are included, since the internal extinction correction of these almost edge-on galaxies, will brighten them above the adopted threshold absolute magnitude.

In columns of Table A2 the following information is presented. Column 1 - the group name, which is either the Tully group (TG) number (for those from Tully et al. 2008), or the name of the brightest member for pairs/triplets/groups from Karachentsev & Makarov (2008); Makarov & Karachentsev (2009) and Makarov & Karachentsev (2011). Columns 2 and 3 - J2000 coordinates of group centre. Column 4 - the group heliocentric velocity; column 5 - V_{LG} , the group velocity relative to the Local Group centre. Column 6 - the group distance velocity V_{dist} , which are taken either from the non-redshift measurements for Tully et al. (2008) sample objects or from V_{LG} with the account for the discussed in Section 2.2 V_{pec} .

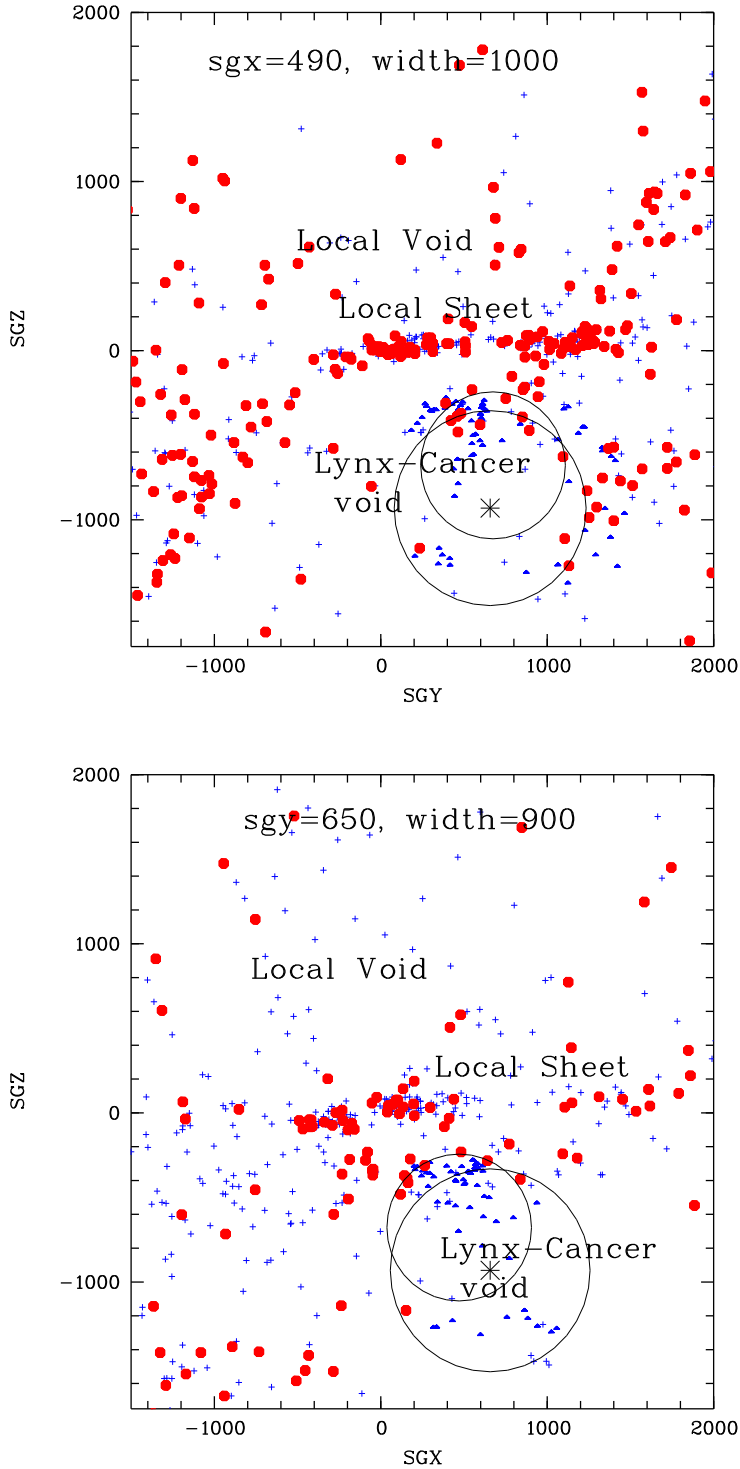


Figure A1. Illustration of the Lynx-Cancer void position relative to the more common elements of the local large-scale structure. *top panel:* the SGY-SGZ (in km s^{-1}) projection of the slice with the centre at $\text{SGX}=490 \text{ km s}^{-1}$ and the width $\Delta\text{SGX}=1000 \text{ km s}^{-1}$. *bottom panel:* the SGX-SGZ (in km s^{-1}) projection of the slice with the centre at $\text{SGY}=650 \text{ km s}^{-1}$ and the width $\Delta\text{SGY}=900 \text{ km s}^{-1}$. The large red octagons represent luminous ($M_B < -19.0$) galaxies. The blue small crosses represent fainter galaxies with the known non-redshift distances from Tully et al. (2008). The blue filled triangles represent (not all) galaxies falling in the Lynx-Cancer void as described in Section 3. The projections of the maximal inscribed spheres for Lynx-Cancer void (main) and the subvoid are shown by the large and small circles. The asterisk marks the centre of the main Lynx-Cancer void. The Inner Local Void of Tully et al. (2008) at the positive SGZ is almost adjacent to the Local Sheet at $\text{SGZ} \approx 0$.

Table A1. List of ‘isolated’ luminous galaxies delineating the Lynx-Cancer void

#	Name (1)	Coordinates (J2000)		V_{hel}	σ_V	V_{LG}	V_{dis}	B_{tot}	A_B	M_B^a	SGXV	SGYV	SGZV	D_{NN}	Notes (15)
		(2)	(3)	(4)	(5)	(6)	(7)	(8)	(9)	(10)	(11)	(12)	(13)	(14)	
1	NGC2543	08 12 58.0	+36 15 17	2471	9	2449	1920	12.86	0.30	-19.54	1102	1125	-1098	4.90	
2	NGC2654	08 49 11.8	+60 13 14	1349	3	1478	1924	12.67	0.28	-19.70	1439	1226	-356	2.55	
3	NGC2880	09 29 34.6	+62 29 27	1608	21	1716	1600	12.46	0.14	-19.38	1157	1091	-171	1.59	
4	NGC3041	09 53 07.2	+16 40 40	1408	2	1271	1829	12.31	0.15	-19.81	208	1476	-1060	2.27	
5	NGC3198	10 19 54.9	+45 32 59	663	4	682	1008	11.07	0.05	-19.68	482	855	-231	1.33	UGC5572
6	NGC3239	10 25 05.7	+17 09 37	753	3	622	912	11.71	0.14	-18.91*	52	798	-438	2.04	UGC5637
7	NGC3319	10 39 09.5	+41 41 13	739	1	740	971	11.48	0.06	-19.20	387	864	-215	1.33	
8	NGC3344	10 43 30.2	+24 55 25	586	4	498	788	10.38	0.14	-19.93	113	726	-284	2.40	UGC 5840
9	NGC3365	10 46 12.6	+01 48 47	986	1	789	1336	13.17	0.20	-18.34*	-294	1116	-674	4.85	
10	NGC3432	10 52 31.0	+36 37 10	613	4	606	1117	11.64	0.06	-19.33	341	1031	-259	2.45	

^a absolute magnitudes are corrected only for Galactic extinction according to NED;

* Almost edge-on galaxies. The account for internal extinction leads to $M_B < -19.0$.

Table A2. Main parameters of groups and pairs delineating the Lynx-Cancer void

#	Name (1)	Coordinates (J2000) (2) (3)		V_{hel}^a (4)	V_{LG}^a (5)	V_{dis}^a (6)	SGXV (7)	SGYV (8)	SGZV (9)	D_{NN} (10)	Notes (11)
1	NGC2273 ^d	06 50 07.4	+60 50 30		1967	2190	1917	928	-509	7.44	NGC2273 -brightest
2	NGC2460 ^c	07 57 02.5	+60 22 38		1558	1723	1388	945	-384	3.62	NGC2460 -brightest
3	IC2267 ^d	08 18 03.4	+24 45 33		1999	2307	977	1315	-1624	6.02	IC2267 -brightest
4	TG 179 ^a	08 18 58.3	+57 48 44	1082	1173	925	708	549	-231	3.02	NGC2549 -brightest
5	TG 579 ^a	08 27 07.0	+25 57 27	2068	1988	1876	790	1130	-1272	4.90	NGC2592 -brightest
6	TG 282 ^a	08 52 41.4	+33 25 19	420	374	581	272	401	-320	2.16	NGC2683 -brightest
7	TG 292 ^a	08 53 24.0	+51 18 54	707	758	1266	844	857	-395	2.38	NGC2681 -brightest
8	NGC2685 ^b	08 55 35.5	+58 44 11		992	1196	872	782	-240	2.21	NGC2685 -brightest
9	TG 167 ^a	09 07 02.5	+60 07 44	1386	1482	1656	1205	1101	-277	1.59	NGC2768 -brightest
10	TG 389 ^a	09 09 33.5	+33 07 25	2028	1978	2221	963	1630	-1162	5.28	NGC2770 -brightest
11	NGC2775 ^b	09 10 20.1	+07 02 17	1350	1169	1491	88	964	-1134	4.12	NGC2775 -brightest
12	NGC2798 ^c	09 17 22.3	+41 59 56		1707	1974	1047	1475	-791	3.20	NGC2798 -brightest
13	NGC2820 ^c	09 21 36.7	+64 15 23		1697	1898	1415	1253	-174	2.55	NGC2820 -brightest
14	NGC2844 ^c	09 21 48.7	+40 09 14		1478	1750	877	1329	-727	2.82	NGC2844 -brightest
15	TG 293 ^a	09 22 01.5	+50 59 30	637	684	1029	642	752	-283	2.29	NGC2841 -brightest
16	NGC2859 ^c	09 24 03.0	+34 30 51	1679	1636	1854	788	1425	-886	2.82	NGC2859 -brightest
17	TG 271 ^a	09 32 09.9	+21 30 00	554	441	615	140	474	-365	2.16	NGC2903 -brightest
18	TG 168 ^a	09 42 35.8	+58 51 08	1362	1451	1090	738	788	-151	2.21	NGC2950 -brightest
19	TG 378 ^a	09 45 13.5	+32 21 53	1461	1403	1634	585	1333	-742	1.36	NGC2964 -brightest
20	TG 401 ^a	09 50 15.0	+12 47 43	1437	1281	1717	104	1347	-1060	2.27	NGC3020 -brightest
21	TG 379 ^a	09 52 08.3	+29 14 11	1499	1427	1628	490	1352	-764	2.13	NGC3032 -brightest
22	TG 373 ^a	09 55 17.8	+04 16 15	1335	1128	1498	-119	1122	-985	4.46	NGC3044 -brightest, NGC3055
23	TG 157 ^a	10 01 59.5	+55 40 04	1126	1199	1413	880	1086	-210	3.85	NGC3079 -brightest
24	NGC3118 ^a	10 07 03.6	+33 00 43	1362	1312	1592	522	1368	-625	1.96	NGC3118 -brightest
25	NGC3184 ^c	10 17 55.2	+41 24 33		592	892	380	768	-248	1.40	NGC3184 -brightest
26	NGC3227 ^b	10 23 41.4	+19 54 48		1034	1552	159	1366	-718	1.45	NGC3227 -brightest
27	TG 370 ^a	10 29 02.5	+28 44 23	1345	1272	1526	346	1374	-567	2.59	NGC3245 -brightest
28	NGC3301 ^b	10 36 25.3	+21 49 35		1219	1504	163	1364	-613	1.45	NGC3301 -brightest
29	NGC3338 ^b	10 42 27.1	+13 57 56		1123	1833	-46	1640	-816	3.76	NGC3338 -brightest
30	TG 266 ^a	10 48 15.7	+12 33 32	819	670	811	-47	729	-353	1.33	M105 group
31	TG 364 ^a	10 48 29.6	+12 31 07	1285	1136	1565	-93	1407	-679	2.04	NGC3373 -brightest
32	TG 268 ^a	10 51 23.2	+05 51 00	1023	844	825	-139	717	-383	1.33	NGC3423 -brightest
33	TG 361	10 56 18.6	+17 30 53	1104		1526	7	1416	-569	2.04	
34	TG 269 ^a	11 00 36.2	+28 58 08	683	620	1000	177	946	-272	2.55	NGC3486 -brightest

^a group coordinates are from Makarov & Karachentsev (2011) [MK11]; ^b ‘groups’ are from MK11, V_{dist} are calculated from V_{LG} and ΔV_{pec} ;^c MK11 groups, absent in Tully sample; ^d MK11 groups with a member(s), from the Tully list. Their V_{dist} are adopted as for the respective galaxies.